

From Dead Pixels to Editable Slides: Infographic Reconstruction into Native Google Slides via Vision-Language Region Understanding

Leonardo Gonzalez

Trilogy AI Center of Excellence
Austin, USA

Abstract

Infographics are widely used to communicate information with a combination of text, icons, and data visualizations, but once exported as images their content is locked into pixels, making updates, localization, and reuse expensive. We describe **IMAGES2SLIDES**, an API-based pipeline that converts a static infographic (PNG/JPG) into a native, editable Google Slides slide by extracting a region-level specification with a vision-language model (VLM), mapping pixel geometry into slide coordinates, and recreating elements using the Google Slides batch update API. The system is model-agnostic and supports multiple VLM backends via a common JSON region schema and deterministic postprocessing. On a controlled benchmark of 29 programmatically generated infographic slides with known ground-truth regions, **IMAGES2SLIDES** achieves an overall element recovery rate of 0.989 ± 0.057 (text: 0.985 ± 0.083 , images: 1.000 ± 0.000), with mean text transcription error CER = 0.033 ± 0.149 and mean layout fidelity IoU = 0.364 ± 0.161 for text regions and 0.644 ± 0.131 for image regions. We also highlight practical engineering challenges in reconstruction, including text size calibration and non-uniform backgrounds, and describe failure modes that guide future work.

CCS Concepts

- Computing methodologies → Computer vision; Machine learning;
- Human-centered computing → Visualization systems and tools.

Keywords

infographic understanding, vision-language models, document layout analysis, chart understanding, structured generation, presentation automation

ACM Reference Format:

Leonardo Gonzalez. 2026. From Dead Pixels to Editable Slides: Infographic Reconstruction into Native Google Slides via Vision-Language Region Understanding. In *Companion Proceedings of the ACM Web Conference 2026 (WWW Companion '26)*, April 13–17, 2026, Dubai, United Arab Emirates. ACM, New York, NY, USA, 7 pages. <https://doi.org/10.1145/3774905.3795609>



This work is licensed under a Creative Commons Attribution 4.0 International License.
WWW Companion '26, Dubai, United Arab Emirates
 © 2026 Copyright held by the owner/author(s).
 ACM ISBN 979-8-4007-2308-7/2026/04
<https://doi.org/10.1145/3774905.3795609>

1 Introduction

Infographics compress complex information into compact visuals that mix dense text, graphical annotations, and small icons or charts. Once exported as raster images, however, they become *dead pixels*: updating labels, correcting numbers, translating text, or repurposing the design for new audiences typically requires redesign work.

Recent progress in vision-language models (VLMs) suggests that screen-like media can be parsed into structured, element-level representations that preserve content and geometry. ScreenAI, for example, targets UIs and infographics and is trained with a screen annotation task that predicts element types and locations [3]. Benchmarks such as DocVQA and InfographicVQA emphasize the need to jointly reason over embedded text and layout [6, 7], while newer suites like MMMU and MMDocBench broaden evaluation across diverse multimodal inputs, including charts and infographics [4, 8]. Separately, “derendering” has emerged as a useful lens for converting visual artifacts into structured, editable representations [16, 25].

This paper presents **IMAGES2SLIDES**, an implemented pipeline that reconstructs a static infographic as a native Google Slides slide using explicit regions and API-driven creation [26]. The core goal is editability: textual content becomes editable slide text objects while preserving layout as closely as possible.

Contributions. We contribute:

- An end-to-end, API-based system that reconstructs an infographic image as an editable Google Slides slide via region extraction, geometry mapping, and structured slide generation [26].
- A lightweight, model-agnostic region schema with deterministic validation and postprocessing, enabling multiple VLM backends (including open-weight alternatives such as Qwen3-VL) [2].
- Practical reconstruction techniques, including deterministic element IDs for retries and a piecewise-linear font size calibration that improves readability of small text.
- A discussion of limitations and workflow strategies for non-uniform backgrounds and raster-only visual elements, informed by related work in document layout analysis and chart understanding [12, 13, 20, 22, 23].
- A quantitative evaluation on a controlled benchmark with programmatically generated ground truth, reporting text accuracy (CER/WER), layout fidelity (IoU and center offset), and editability recovery rates.

2 Related Work

Our approach relates to three research threads: (i) multimodal understanding of documents and infographics; (ii) region extraction and layout reconstruction; and (iii) visual-to-structured generation and derendering.

Multimodal document and infographic understanding. Document VQA benchmarks highlight the interaction between layout, text, and visuals [6, 7]. General multimodal benchmarks like MMMU test broad perception and reasoning, including diagram and chart-style inputs [8]. MMDocBench provides OCR-free document tasks with supporting regions, enabling fine-grained evaluation of localization and extraction in charts and infographics [4]. Model-side work addresses the difficulty of reading text-rich images: DocOwl 1.5 emphasizes structure learning for OCR-free document understanding [19], while DocVLM augments frozen VLMs with OCR-derived text and layout as learned queries to reduce reliance on high-resolution visual tokens [5]. ScreenAI focuses specifically on UIs and infographics and uses element-level supervision for types and locations [3].

Region extraction and layout reconstruction. Document layout analysis decomposes pages into regions and reading order, providing a basis for conversion and retrieval. Large datasets such as PubLayNet and DocLayNet enable scalable training and evaluation of layout detectors [11, 12]. Tooling such as LayoutParser streamlines application of deep layout models [14]. End-to-end approaches like DLAFormer integrate multiple layout subtasks in a transformer architecture by casting detection, classification, and ordering as relation prediction [13]. Complementary work on multimodal document pretraining, such as LayoutLM/LayoutLMv3 and UDOP, unifies text, layout, and vision signals for downstream document tasks [9, 10, 17].

Visual-to-structured generation and derendering. OCR-free sequence generation approaches such as Donut output structured representations directly from document images [15]. Nougat focuses on converting scientific PDFs into structured markup, recovering layout-dependent semantics like math [18]. Pix2Struct uses screenshot parsing as pretraining, learning to map masked screenshots to simplified HTML [16]. In chart-specific settings, ChartQA benchmarks question answering over charts [20], and models such as MatCha, DePlot, UniChart, and ChartReader study chart derendering and chart-to-structured representations [21–24]. Design2Code benchmarks multimodal generation of front-end code from visual designs [25]. We adopt a related perspective but target the Google Slides object model as the structured output.

3 Problem Formulation

Given an infographic image I with pixel dimensions (W_I, H_I) , we aim to produce a Google Slides slide S containing a set of page elements $\{e_k\}$ such that:

- (1) **Editability:** text in I is recreated as editable slide text objects.
- (2) **Layout fidelity:** the spatial arrangement of elements approximates the original infographic geometry.
- (3) **Practicality:** the pipeline is robust to varied infographic styles and supports iterative refinement.

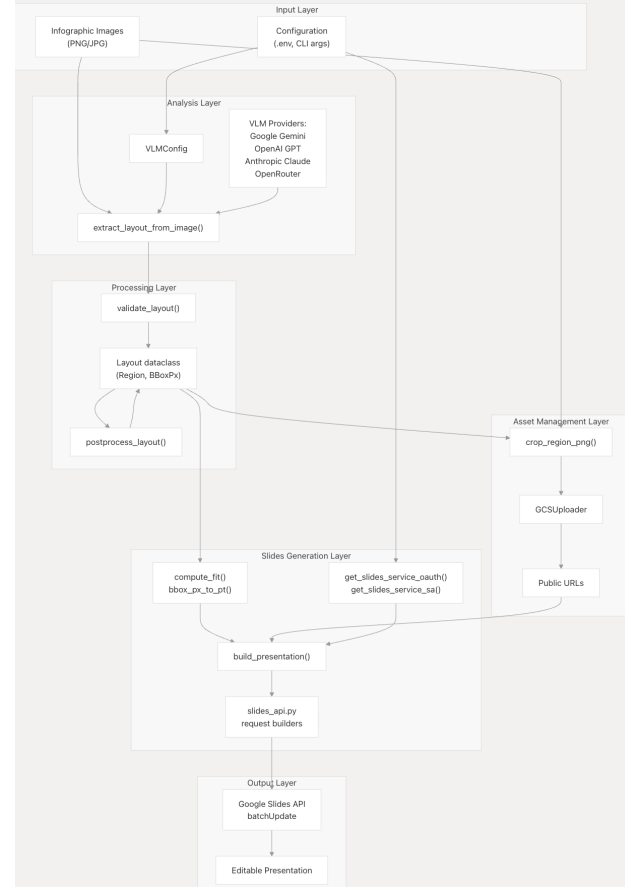


Figure 1: Layered architecture of IMAGES2SLIDES. The pipeline is organized into input, analysis, processing, asset management, slides generation, and output layers.

We represent infographic structure as a region file \mathcal{R} , produced by a VLM and validated by deterministic postprocessing. Each region includes an ID; a type (text or image); a pixel bounding box; optional reading order and tags; extracted text for text regions; and optional style hints and confidence.

4 System Overview

Figure 1 summarizes the modular architecture of IMAGES2SLIDES. Table 1 summarizes the data flow.

4.1 VLM-based region extraction

We prompt a VLM to produce a strict JSON region file \mathcal{R} with pixel-space coordinates, region types, and extracted text. The prompt emphasizes explicit image dimensions, well-scoped regions, stable IDs, and reading order and tags when available. This aligns with element-centric screen understanding [3] and region-grounded evaluation in document benchmarks [4].

Table 1: Data flow through the pipeline (stages, artifacts, and outputs).

Stage	Input	Processing	Output
1. VLM analysis	Infographic image (PNG/JPG)	extract_layout_from_image() using a selected VLM backend and a strict JSON schema (regions, types, bboxes, text).	Raw JSON layout (text and image regions)
2. Validation & post-process	Raw JSON layout	validate_layout() converts JSON to typed objects; postprocess_layout() normalizes text, clamps boxes, applies minimal heuristics for consistency.	Clean, typed Layout object
3. Asset prep	Image + Layout	For each image region: crop_region_png() (with small padding) and upload to obtain an HTTPS-accessible URL.	Public URLs for image regions
4. Geometry	Layout + slide page size	compute_fit() preserves aspect ratio and centers the image; bbox_px_to_pt() maps pixel boxes to slide points.	Slide coordinates (pt) for all regions
5. API requests	Coordinates + asset URLs	build_requests_for_infographic() constructs a single Slides API batch (create slide, add text boxes, insert text, place images).	Slides API request batch
6. Execution	Request batch	presentations.batchUpdate applies the batch to the target presentation.	Live, editable Google Slides presentation

4.2 Region JSON schema

To support reliable reconstruction across model backends, IMAGES2SLIDES uses a strict, typed region schema that distinguishes two region types: text and image. Both include pixel-space geometry, while text regions also carry extracted text and optional font/style hints, and image regions specify only the coordinates used to crop the source image. The top-level JSON contains image dimensions and a list of regions:

Listing 1: Top-level layout schema (abridged).

```
{
  "image_px": {
    "width": 1600,
    "height": 900
  },
  "regions": [
    {
      "id": "title",
      "order": 1,
      "type": "text",
      "bbox_px": {
        "x": 35.0,
        "y": 45.0,
        "w": 1500.0,
        "h": 60.0
      },
      "text": "The Psychology of Buying: 3 Triggers Driving E-Commerce Sales",
      "style": {
        "font_family": "Arial",
        "font_size_pt": 42,
        "bold": true
      },
      "crop_from_infographic": false,
      "confidence": 0.99,
      "notes": null
    },
    {
      "id": "image_social_proof",
      "order": 2,
      "type": "image",
      "bbox_px": {
        "x": 32.0,
        "y": 140.0,
        "w": 469.0,
        "h": 351.0
      },
      "text": null,
      "style": null,
      "crop_from_infographic": true,
      "confidence": 0.98,
      "notes": "Includes smartphone illustration and background container"
    }
  ]
}
```

Table 2: Region schema (abridged) and validation rules.

Field	Description / constraints
id	Required. Stable identifier (string) used for deterministic object IDs in Slides (e.g., TXT_<id>).
order	Required. Reading order hint (integer); fallback ordering is computed if missing.
type	Required. One of {text, image}.
bbox_px	Required. Pixel-space box {x, y, w, h} in the input image coordinate system; clamped to image bounds; requires w, h > 0.
text	Required for type=text. Must be non-empty after whitespace normalization.
style	Optional style hints (e.g., font_family, font_size_pt, bold); missing fields fall back to defaults.
crop_from_infographic	Optional boolean. If true, the pipeline crops the region from the original infographic and inserts it as an image object.
confidence, notes	Optional. Confidence in [0, 1] and free-form notes for debugging.

```

  }
]
```

Table 2 summarizes the region object fields and key constraints enforced during validation and postprocessing.

We constrain prompting to improve parseability: the model must output *JSON only* (no Markdown or commentary), include exact image dimensions, keep all boxes within bounds, and avoid inferring or fabricating text that is not visible in the image.

The implementation supports multiple VLM providers behind a unified interface, including Google Gemini [1], OpenAI GPT, Anthropic Claude, and OpenRouter-hosted models (e.g., Qwen3-VL) [2]. To improve robustness, malformed or schema-violating JSON responses are detected during validation and can trigger a retry with error feedback describing the expected schema.

4.3 Layout postprocessing

Model outputs can contain minor inconsistencies (e.g., empty strings, boxes outside bounds). We apply deterministic postprocessing:

whitespace normalization, bounds clamping, minimum size enforcement, and fallback ordering (top-to-bottom, left-to-right). Intermediate artifacts (raw JSON, validated JSON, rendered debug overlays) are cached to support rapid iteration.

4.4 Geometry mapping

Slides use page coordinates in points, while regions are defined in pixels. Object geometry is expressed via size and affine transforms in the Slides API [27]. We fit the infographic into the slide while preserving aspect ratio and compute a scale factor and centering offsets. Let slide page size be (W_S, H_S) in points, and image size be (W_I, H_I) in pixels:

$$s = \min\left(\frac{W_S}{W_I}, \frac{H_S}{H_I}\right), \quad (1)$$

$$\Delta_x = \frac{W_S - sW_I}{2}, \quad \Delta_y = \frac{H_S - sH_I}{2}. \quad (2)$$

A region with pixel box (x, y, w, h) maps to slide rectangle $(x', y', w', h') = (\Delta_x + sx, \Delta_y + sy, sw, sh)$.

4.5 Slide reconstruction via Google Slides API

We create and populate slides using `presentations.batchUpdate` [26]. The pipeline issues a batch of API requests to create a slide, add text boxes, insert text, and apply text styling. For image regions, we crop the region from the original infographic, upload it to an HTTPS-accessible URL, and place it as an image element.

Deterministic IDs for retries. To support retries and incremental updates, the system uses deterministic object IDs derived from region IDs (e.g., `TXT_<id>`, `IMG_<id>`).

5 Typography Calibration

In practice, VLM-based region extraction tends to underestimate font sizes, especially for small body text and labels. Because slide geometry is scaled from image pixels into slide points, the system first derives a base font size in points, $f = f_{\text{vlm}} \cdot s$, where f_{vlm} is the model-provided estimate and s is the image-to-slide scale factor used for placement.

5.1 Piecewise-linear font scaling

We apply a piecewise-linear calibration that boosts smaller fonts while leaving large titles unchanged. Let f be the base font size (in points). The calibrated size is:

$$f' = f + \max(0, (14 - f) \times 0.294). \quad (3)$$

This function has two anchor behaviors that match the implemented workflow: (i) small body text at 5.5 pt is increased to 8 pt (a readable minimum in many slide contexts), and (ii) text at 14 pt and above is left unchanged. Below 14 pt, the mapping is linear and provides larger relative boosts to smaller fonts.

5.2 Collision-aware text box width expansion

Increasing font size can increase the rendered line length and cause overflow within a fixed-width text box. To mitigate this, we optionally expand the text box width in proportion to the font scaling factor while preventing overlap with neighboring regions:

(1) Compute the font ratio $r = f'/f$.

- (2) Compute a desired width $w'_{\text{desired}} = w' \cdot r$ (where w' is the mapped box width in points).
- (3) Initialize the candidate right edge $right = x' + w'_{\text{desired}}$.
- (4) Cap $right$ to the slide boundary with a small margin.
- (5) If there is a neighboring region to the right whose vertical span overlaps this text box, cap $right$ to that region's left edge minus a small gap.
- (6) Set the adjusted width $w'_{\text{adj}} = \max(w', right - x')$ while keeping the left edge x' fixed.

This preserves alignment while reducing overflow and avoiding collisions in dense layouts.

6 Image Region Handling

Non-text regions (icons, logos, small diagrams, and chart insets) are handled as raster assets: we crop the region from the source infographic and place it as an image element in Slides.

6.1 Crop padding

VLMs often produce tight bounding boxes that can clip strokes or antialiased edges. We therefore pad the crop on the right and bottom edges by a small fixed amount (10 px in the current implementation), clamped to image bounds:

$$x_2 = \min(x + w + 10, W_I), \quad (4)$$

$$y_2 = \min(y + h + 10, H_I). \quad (5)$$

The top-left corner (x, y) is preserved to maintain alignment with overlaid elements.

6.2 Upload and deduplication

The Google Slides API creates images from URLs, so cropped assets must be uploaded to an HTTPS-accessible location before slide creation [26]. To reduce redundant uploads and improve reproducibility, cropped images are stored with content-addressed names (a hash of the image bytes), enabling deduplication and caching across runs.

7 Background Handling

Non-uniform or textured backgrounds complicate reconstruction, particularly when the goal is a clean, editable slide. `IMAGES2SLIDES` optionally synthesizes a clean background from the infographic when the `-synthesize-background` flag is enabled. The pipeline prompts a VLM to return a `background_sample` JSON object with a pixel-space box and a mode label: `solid` for near-uniform backgrounds or `tile` for textured/patterned ones. We crop the sampled patch and generate a full-size background image by either (i) filling the slide with the patch's average color (`solid`) or (ii) tiling the patch across the slide (`tile`). The synthesized background is uploaded and inserted as a single image element, then editable text and cropped region images are placed above it.

When background synthesis is disabled, we omit the background entirely and reconstruct only extracted text and image regions to avoid duplicating foreground content.

Table 3: Quantitative evaluation on 29 programmatically generated infographic slides. Values are mean \pm std across runs.

Metric	Text	Image	Overall / global
Element recovery rate	0.985 ± 0.083	1.000 ± 0.000	0.989 ± 0.057
Character recovery rate	0.969 ± 0.124	–	–
Mean IoU	0.364 ± 0.161	0.644 ± 0.131	–
Median IoU	0.388 ± 0.177	0.639 ± 0.130	–
Mean center offset (px)	53.7 ± 26.9	11.0 ± 16.3	–
Mean CER / WER	$0.033 \pm 0.149 / 0.037 \pm 0.167$	–	–
Frac. IoU ≥ 0.5	0.376 ± 0.292	0.871 ± 0.332	0.513 ± 0.237
Frac. IoU ≥ 0.75	0.031 ± 0.092	0.181 ± 0.362	0.071 ± 0.110
VLM extraction time (s)		54.999 ± 18.337	
Slides API time (s)		5.792 ± 0.682	

8 Evaluation

A common challenge in evaluating raster-to-editable pipelines is obtaining ground-truth element geometry. To avoid manual labeling, we use a controlled round-trip benchmark that programmatically generates ground-truth Slides with known region coordinates, rasterizes them, and then reconstructs them with IMAGES2SLIDES.

8.1 Benchmark construction

Each evaluation run generates a synthetic infographic slide by (i) sampling a grid/panel layout template, (ii) prompting a text VLM to produce a cohesive infographic concept and a region JSON specification conforming to our schema (Section 4.2), and (iii) generating the referenced images with a text-to-image model. The ground-truth slide is created using the same Slides generation functions as IMAGES2SLIDES, ensuring that region boxes correspond to known pixel coordinates in the exported PNG. We then export the slide as a raster image and feed it to IMAGES2SLIDES to obtain a predicted region JSON and an editable reconstructed slide.

We report results over 29 successfully completed runs (provider: Google Gemini backend), with each run producing a single 1600×900 infographic image and paired ground truth and prediction `gt_region.json` and `pred_region.json` files.

We report quantitative results for a single backend to provide a concrete reference point; the benchmarking harness is backend-agnostic and can be rerun with alternative providers. We include wall-clock time for the VLM and Slides API stages. Future work could log input/output token counts from provider response metadata, where available, to enable post-hoc cost estimation.

8.2 Metrics

We evaluate three aspects of reconstruction:

- **Editability recovery.** Element recovery rate is the fraction of ground-truth regions that are matched by a predicted region of the same type. We also compute character recovery rate, the fraction of ground-truth characters recovered across matched text regions.
- **Layout fidelity.** For each matched region we compute bounding-box Intersection-over-Union (IoU) in pixel space and center-point displacement (in pixels and normalized by image diagonal).
- **Text accuracy.** For matched text regions we compute character error rate (CER) and word error rate (WER) via Levenshtein distance.

Predicted regions are matched to ground-truth regions using a one-to-one assignment within each region type that maximizes overlap (IoU); unmatched predictions are counted as false positives, and unmatched ground-truth regions as false negatives.

8.3 Results

Table 3 summarizes mean and standard deviation across runs. Overall element recovery is high (0.989 ± 0.057), with perfect image-region recovery and occasional text-region over-segmentation (false positives) or misses (false negatives). Layout fidelity is stronger for image regions than for text regions, consistent with the fact that small changes in font metrics, line breaking, and text box width can produce low IoU even when transcription is correct.

Across all matched elements (globally aggregated), 37.6% of text boxes and 85.1% of image boxes achieve $\text{IoU} \geq 0.5$, while 2.8% of text boxes and 15.8% of image boxes achieve $\text{IoU} \geq 0.75$. Mean transcription error is low ($\text{CER } 0.033 \pm 0.149$, $\text{WER } 0.037 \pm 0.167$), but variance indicates that a minority of runs still incur noticeable recognition errors (typically stylized or low-contrast text).

8.4 Failure modes

We observed recurring failure patterns that explain most residual errors:

Table 4: Observed failure modes and mitigations.

Failure mode	Symptom and mitigation
Text over-segmentation	A single paragraph is split into multiple regions, increasing false positives and lowering IoU. Mitigation: merge adjacent text boxes with compatible styles and small gaps.
Text under-segmentation	Multiple logical blocks are merged, harming editability. Mitigation: split using OCR line clustering or whitespace-based heuristics.
Font metric mismatch	Correct text but incorrect line breaks and box sizes reduce IoU. Mitigation: font calibration (Section 5) and collision-aware width expansion.
Low contrast / stylized text	Non-zero CER/WER in runs with decorative typography or low resolution. Mitigation: upscale preprocessing, contrast enhancement, or fallback to OCR for text regions.
Non-uniform backgrounds	Decorative containers or gradients complicate clean reconstruction. Mitigation: VLM-guided background sampling and synthesized background tiling/fill (Section 7).

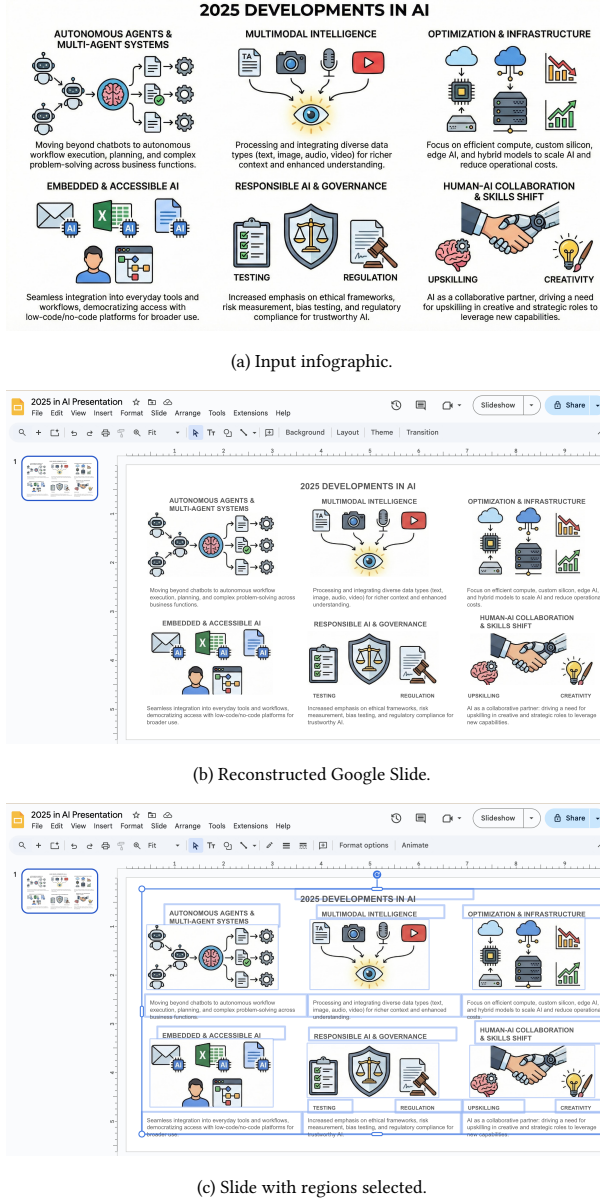


Figure 2: End-to-end example reconstruction produced by IMAGES2SLIDES.

8.5 Qualitative example

Figure 2 illustrates a representative end-to-end reconstruction: the input infographic, the reconstructed Google Slides slide, and the same slide with all reconstructed regions selected to visualize element boundaries.

9 Discussion and Limitations

Raster-to-native gap. The pipeline prioritizes editability of text and placement of raster visual elements. It does not fully reconstruct complex vector primitives (custom shapes, gradients, rich charts)

as native slide objects. Chart-specific derendering methods [21–24] suggest a path toward future chart-to-native regeneration.

Dependence on region quality. Reconstruction quality depends on the region specification. Layout and structure learning methods [5, 13, 19] motivate improvements in localization fidelity and ordering that could directly benefit reconstruction.

Operational constraints. The Slides API requires publicly accessible URLs for images, which introduces an asset-hosting component in end-to-end automation [26].

10 Ethical Considerations

This work can be applied to copyrighted or sensitive visual content; deployments should respect content provenance, licensing, and privacy. When used with generated infographics, systems should disclose synthetic origins and avoid deceptive presentation.

11 Artifact Availability

Code, evaluation scripts, and assets are available at <https://github.com/kumanday/images2slides>.

12 Conclusion

We presented IMAGES2SLIDES, an implemented pipeline for converting static infographic images into native, editable Google Slides slides via VLM-based region extraction and API-driven reconstruction. The approach bridges document-style visual understanding and practical visualization authoring, emphasizing editability and workflow usability. We documented engineering techniques that improve reconstruction in practice, particularly for typography and backgrounds.

References

- [1] R. Doshi. Gemini 3 Pro: the frontier of vision AI. Google Blog, 2025. <https://blog.google/innovation-and-ai/technology/developers-tools/gemini-3-pro-vision/>.
- [2] S. Bai et al. Qwen3-VL Technical Report. *arXiv:2511.21631*, 2025. <https://arxiv.org/abs/2511.21631>.
- [3] G. Baechler, S. Sunkara, M. Wang, F. Zubach, H. Mansoor, V. Etter, V. Cărbune, J. Lin, J. Chen, and A. Sharma. ScreenAI: A Vision-Language Model for UI and Infographics Understanding. *arXiv:2402.04615*, 2024. <https://arxiv.org/abs/2402.04615>.
- [4] F. Zhu, Z. Liu, X. Y. Ng, H. Wu, W. Wang, F. Feng, C. Wang, H. Luan, and T. S. Chua. MMDocBench: Benchmarking Large Vision-Language Models for Fine-Grained Visual Document Understanding. *arXiv:2410.21311*, 2024. <https://arxiv.org/abs/2410.21311>.
- [5] M. Shpigel Nacson et al. DocVLM: Make Your VLM an Efficient Reader. *arXiv:2412.08746*, 2024. <https://arxiv.org/abs/2412.08746>.
- [6] M. Mathew, V. Bagal, R. P. Tito, D. Karatzas, E. Valveny, and C. V. Jawahar. InfographicVQA. In *Proc. WACV*, 2022. <https://arxiv.org/abs/2104.12756>.
- [7] M. Mathew, D. Karatzas, and C. V. Jawahar. DocVQA: A Dataset for VQA on Document Images. In *Proc. WACV*, 2021. <https://arxiv.org/abs/2007.00398>.
- [8] X. Yu et al. MMMU: A Massive Multi-discipline Multimodal Understanding and Reasoning Benchmark for Expert AGI. In *Proc. CVPR*, 2024. <https://arxiv.org/abs/2311.16502>.
- [9] Y. Huang, T. Lv, L. Cui, Y. Lu, and F. Wei. LayoutLMv3: Pre-training for Document AI with Unified Text and Image Masking. *arXiv:2204.08387*, 2022. <https://arxiv.org/abs/2204.08387>.
- [10] Y. Xu et al. LayoutLM: Pre-training of Text and Layout for Document Image Understanding. In *Proc. ACM KDD*, 2020. <https://arxiv.org/abs/1912.13318>.
- [11] B. Fitzmann et al. DocLayNet: A Large Human-Annotated Dataset for Document-Layout Analysis. *arXiv:2206.01062*, 2022. <https://arxiv.org/abs/2206.01062>.
- [12] X. Zhong, J. Tang, and A. Jimeno Yepes. PubLayNet: Largest Dataset Ever for Document Layout Analysis. In *Proc. ICDAR*, 2019. <https://arxiv.org/abs/1908.07836>.

- [13] J. Wang, K. Hu, and Q. Huo. DLAFormer: An End-to-End Transformer for Document Layout Analysis. *arXiv:2405.11757*, 2024. <https://arxiv.org/abs/2405.11757>.
- [14] Z. Shen et al. LayoutParser: A Unified Toolkit for Deep Learning Based Document Image Analysis. *arXiv:2103.15348*, 2021. <https://arxiv.org/abs/2103.15348>.
- [15] G. Kim et al. OCR-free Document Understanding Transformer. *arXiv:2111.15664*, 2021. <https://arxiv.org/abs/2111.15664>.
- [16] K. Lee et al. Pix2Struct: Screenshot Parsing as Pretraining for Visual Language Understanding. *arXiv:2210.03347*, 2022. <https://arxiv.org/abs/2210.03347>.
- [17] Z. Tang et al. Unifying Vision, Text, and Layout for Universal Document Processing. In *Proc. CVPR*, 2023. <https://arxiv.org/abs/2212.02623>.
- [18] L. Blecher et al. Nougat: Neural Optical Understanding for Academic Documents. *arXiv:2308.13418*, 2023. <https://arxiv.org/abs/2308.13418>.
- [19] A. Hu et al. mPLUG-DocOwl 1.5: Unified Structure Learning for OCR-free Document Understanding. *arXiv:2403.12895*, 2024. <https://arxiv.org/abs/2403.12895>.
- [20] A. Masry et al. ChartQA: A Benchmark for Question Answering about Charts with Visual and Logical Reasoning. *arXiv:2203.10244*, 2022. <https://arxiv.org/abs/2203.10244>.
- [21] F. Liu et al. MatCha: Enhancing Visual Language Pretraining with Math Reasoning and Chart Derendering. *arXiv:2212.09662*, 2022. <https://arxiv.org/abs/2212.09662>.
- [22] F. Liu et al. DePlot: One-shot Visual Language Reasoning by Plot-to-Table Translation. *arXiv:2212.10505*, 2022. <https://arxiv.org/abs/2212.10505>.
- [23] A. Masry et al. UniChart: A Universal Vision-language Pretrained Model for Chart Comprehension and Reasoning. *arXiv:2305.14761*, 2023. <https://arxiv.org/abs/2305.14761>.
- [24] Z.-Q. Cheng et al. ChartReader: A Unified Framework for Chart Derendering and Comprehension without Heuristic Rules. *arXiv:2304.02173*, 2023. <https://arxiv.org/abs/2304.02173>.
- [25] C. Si et al. Design2Code: Benchmarking Multimodal Code Generation for Automated Front-End Engineering. *arXiv:2403.03163*, 2024. <https://arxiv.org/abs/2403.03163>.
- [26] Google. Google Slides API Documentation. <https://developers.google.com/workspace/slides>. Accessed: 2026-01-14.
- [27] Google. Affine transforms in the Google Slides API. <https://developers.google.com/workspace/slides/api/concepts/transforms>. Accessed: 2026-01-14.